The Plant Cell, Vol. 7, 1129–1142, August 1995

A Family of Transcripts Encoding Water Channel Proteins: Tissue-Specific Expression in the Common Ice Plant

Shigehiro Yamada,[a,1] Maki Katsuhara,[a,2] Walter B. Kelly,[b] Christine B. Michalowski,[a] and Hans J. Bohnert[a,c,d,3]

[a] Department of Biochemistry, University of Arizona, Tucson, Arizona 85721
[b] Department of Biology, University of California at San Diego, La Jolla, California 92093-0116
[c] Department of Molecular and Cellular Biology, University of Arizona, Tucson, Arizona 85721
[d] Department of Plant Sciences, University of Arizona, Biosciences West, Tucson, Arizona 85721

Seawater-strength salt stress of the ice plant (*Mesembryanthemum crystallinum*) initially results in wilting, but full turgor is restored within ~2 days. We are interested in a mechanistic explanation for this behavior and, as a requisite for in-depth biochemical studies, have begun to analyze gene expression changes in roots coincident with the onset of stress. cDNAs that suggested changes in mRNA amount under stress were found; their deduced amino acid sequences share homologies with proteins of the *Mip* (major intrinsic protein) gene family and potentially encode aquaporins. One transcript, *MipB*, was found only in root RNA, whereas two other transcripts, *MipA* and *MipC*, were detected in roots and leaves. Transcript levels of *MipB* were of low abundance. All transcripts declined initially during salt stress but later recovered to at least prestress level. The most drastic decline was in *MipA* and *MipC* transcripts. *MipA* mRNA distribution in roots detected by in situ hybridization indicated that the transcript was present in all cells in the root tip. In the expansion zone of the root where vascular bundles differentiate, *MipA* transcript amounts were most abundant in the endodermis. In older roots, which had undergone secondary growth, *MipA* was highly expressed in cell layers surrounding individual xylem strands. *MipA* was also localized in leaf vascular tissue and, in lower amounts, in mesophyll cells. Transcripts for *MipB* seemed to be present exclusively in the tip of the root, in a zone before and possibly coincident with the development of a vascular system. *MipA*- and *MipB*-encoded proteins expressed in Xenopus oocytes led to increased water permeability. mRNA fluctuations of the most highly expressed *MipA* and *MipC* coincided with turgor changes in leaves under stress. As the leaves regained turgor, transcript levels of these water channel proteins increased.

INTRODUCTION

Water supply under conditions of osmotic stress is crucial for turgor maintenance. A decline of turgor in aboveground meristems leads, at least temporarily, to growth retardation or arrest. Plants have evolved mechanisms to avoid water stress–related growth inhibition, seemingly by increasing cellular internal osmotic pressure by, for example, accumulating part of the assimilated carbon in an osmotically active form, such as sugars, polyols, amino acids, and secondary/tertiary amines (Yancey et al., 1982; McCue and Hanson, 1990; Delauney and Verma, 1993; Tarczynski et al., 1993). Such accumulation, especially if it were rapidly inducible, would lead—in the absence of transpiratory water loss—to an increased osmotic potential in cells in which the accumulation of metabolites would occur. One may assume that additional mechanisms that regulate membrane resistance to water movement between cells are at different osmotic levels. Such mechanisms might facilitate uptake in the root system and/or increase long-distance metabolite and water flux in the absence of transpiratory water losses to meristematic tissues. We are using a plant model, the common ice plant (*Mesembryanthemum crystallinum*), because in this halophyte the initial shock of an extreme lack of water and a subsequent recovery from water stress can be separated experimentally.

Environmental stress in the ice plant during a specific window in the plant's development elicits strong transcriptional induction of sets of genes whose translation products facilitate adaptation of the plant to salt stress, drought, and low temperature (Bohnert et al., 1994; Cushman and Bohnert, 1995). Not all stress responses can be elicited in young plants, and in old plants several responses are constitutive, indicating that the plant's developmental phase changes include the utilization of different biochemical pathways (Vernon and Bohnert, 1992; Cushman and Bohnert, 1995). In addition, not all stresses influence every pathway switch in a similar fashion (Vernon et al., 1993). All reactions to stress, however, lead

[1] Permanent address: Japan Tobacco Inc., Plant Breeding and Genetics Laboratory, 700 Higashibara, Toyoda, Iwata, Shizuoka 438, Japan.
[2] Permanent address: Research Institute for Bioresources, Okayama University, 20-1, chuo-2-chome, Kurashiki, 710 Japan.
[3] To whom correspondence should be addressed.

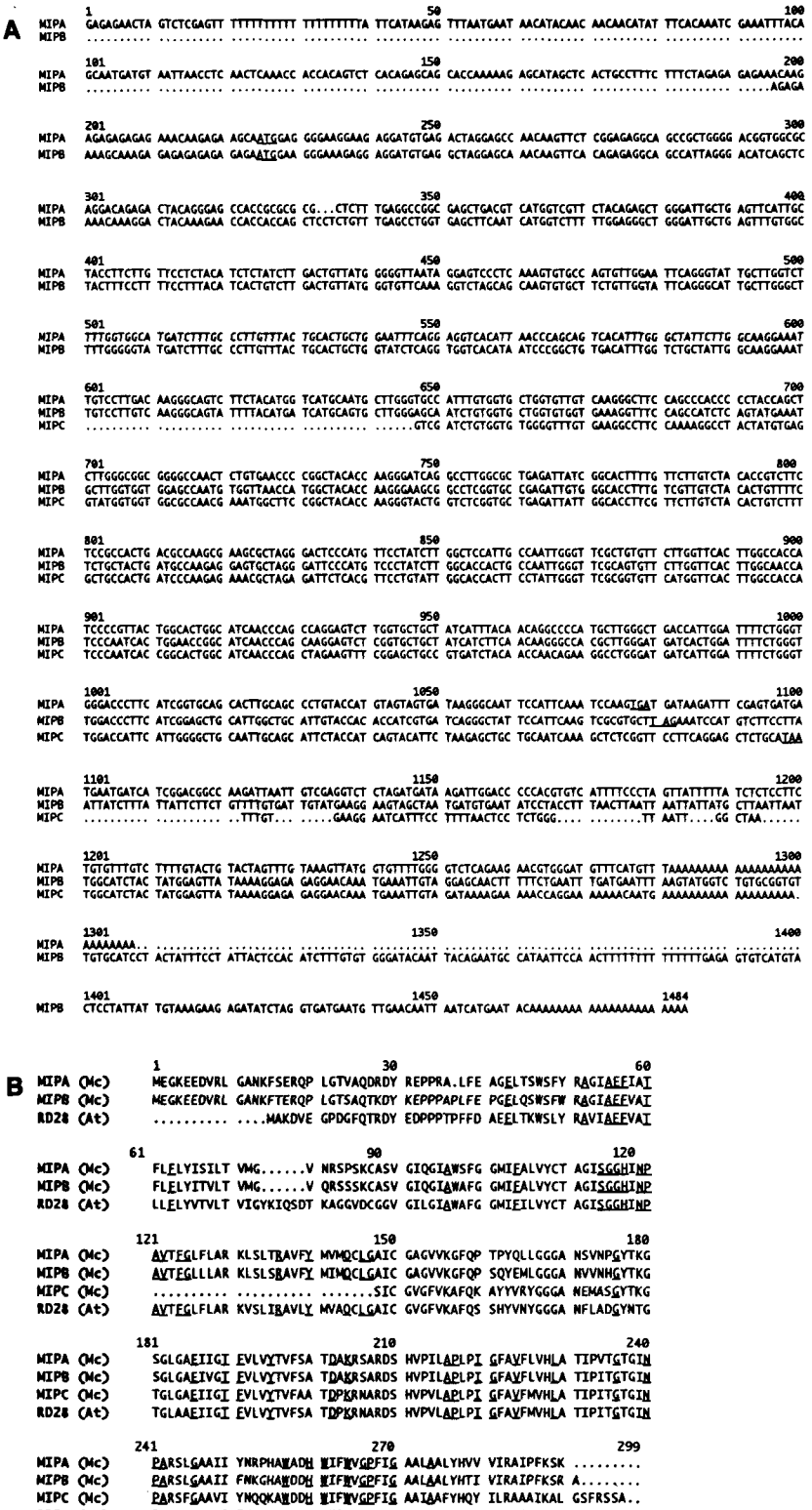

Figure 1. Nucleotide Sequences of *MipA*, *MipB*, and *MipC* Transcripts.

to similar changes in morphology and ultimately to flower evocation in this plant. We find salt stress by NaCl concentrations of seawater strength the most reliable trigger to bring about fast and reproducible changes in the plant's gene expression and development programs and biochemical and physiological reactions.

A sudden increase in NaCl, for example, to 400 mM in hydroponic tanks, leads to almost instantaneous loss of turgor. However, within <2 days, turgor is reestablished. This is in contrast with the behavior of glycophytic plants under comparable severe stress. Part of the turgor restoration seems due to the induction of genes whose translation products promote the production of osmotically active substances, such as D-ononitol, D-pinitol (Vernon and Bohnert, 1992), and proline (Adams et al., 1992; Thomas et al., 1992), which accumulate mainly in growing tissues of the ice plant. Longer term responses include the buildup of Crassulacean acid metabolism, due to the ability of the plants to utilize a stress-inducible phospho*enol*-pyruvate carboxylase isoform as the primary CO_2-fixing enzyme at night (Cushman et al., 1989; Cushman and Bohnert, 1995). Crassulacean acid metabolism is a strategy that reduces water loss. Another long-term stress-relieving mechanism may be seen in the appearance of epidermal bladder cells. Deposition of Na^+ and Cl^- into the vacuoles of these cells permits continued water uptake in the absence of transpiration, which is restricted once the plants have switched to Crassulacean acid metabolism. However, the mechanisms by which the initial loss of turgor is so rapidly overcome following salt shock remain to be identified. We have noted that concentrations of Na^+ and Cl^- in excess of 1 M are found in the ice plant (Adams et al., 1992) and apparently do not constitute salt stress. We consider sodium compartmentation and osmolyte biosynthesis to be the response of the plant to the problem of water availability. This seems to be different from reactions of glycophytes to high concentrations of salt.

Recently, genes have been described that are members of a large superfamily of transmembrane facilitators with the capability of transporting a variety of small molecules, including water, across membranes (Pao et al., 1991; Reizer et al., 1993; Chrispeels and Agre, 1994). Members of the family were first detected in animals in which one protein makes up a major portion of the eye lens, leading to the term major intrinsic protein (MIP; Gorin et al., 1984). When involved in water transport, MIPs are termed aquaporins. In plants, related transcripts and proteins have been found that localize to the tonoplast membrane (Johnson et al., 1990; Höfte et al., 1992). For one of these, tonoplast intrinsic protein (TIP), a function in water transport has been demonstrated (Maurel et al., 1993). More recently, the existence of aquaporins has also been documented for the plasma membrane (Daniels et al., 1994; Kammerloher et al., 1994). These proteins could be involved in plant turgor maintenance, whereas their homologs in animals seem to be involved in excretory functions (Preston and Agre, 1991; Fushimi et al., 1993; Zhang et al., 1993). We have obtained and characterized transcripts, some being only partial sequences, of members of a family of MIP-related genes that function as water channels and show tissue-specific expression and transcript accumulation that are correlated with turgor recovery following salt-induced water stress.

RESULTS

Detection of *Mip* Homologs and Sequence Comparisons

Differential screening of a root cDNA library from ice plants, which had been stressed by the addition of 400 mM NaCl to nutrient solution in hydroponic tanks, indicated that the relative amounts of a number of transcripts changed under stress. Exploratory partial DNA sequence analysis of cDNAs (C.B. Michalowski, unpublished data) indicated that transcripts were present, with their products encoding transmembrane proteins of the MIP family. These proteins have been implicated in water and metabolite transport (Maurel et al., 1993; Reizer et al., 1993; Daniels et al., 1994; Kammerloher et al., 1994). Based on their homology with other sequences (Devereux et al., 1985), we tentatively termed these transcripts *Mip*. From root and leaf cDNA libraries, several apparently full-length and partial cDNAs were subsequently characterized. They indicated that at least five different transcripts of this type exist in *Mesembryanthemum*. Figure 1 shows the sequences of three transcripts. An abundant transcript, *MipA*, encodes a reading frame of 281

Figure 1. (continued).

MipA and *MipB* are full-length transcripts; *MipC* is a partial DNA sequence. Sequence analysis indicated the presence of six putative transmembrane regions with the sequence signature of MIP identified by the Genetics Computer Group program domain search. Excluding the poly(A) stretches, *MipA* is 1272 nucleotides long and *MipB* is 1267 nucleotides long.

(A) An alignment of the three sequences is shown; the initiation codons of *MipA* and *MipB* and the three stop codons are underlined. Dots indicate gaps that distinguish the sequences and a portion that is not available from the partial sequence of *MipC* (EMBL and SwissProt accession numbers: *MipA*, L36095; *MipB*, L36097; *MipC*, L36096).

(B) Alignment of deduced amino acid sequences of MIPA, MIPB, and MIPC for the ice plant (Mc) in comparison with the deduced amino acid sequence of the homologous protein RD28 from Arabidopsis (At) (GenBank accession number D13254/P30302; Yamaguchi-Shinozaki et al., 1992). Underlined are proteins of the TIP family and amino acids that are conserved among the sequences shown. Dots indicate gaps introduced for alignment. Identities at the level of nucleotide and amino acid sequences, respectively, are as follows: MIPA and MIPB, 77.9 and 87.3%, respectively; MIPA and MIPC, 74.6 and 73.9%, respectively; MIPB and MIPC, 70.6 and 73.2%, respectively.

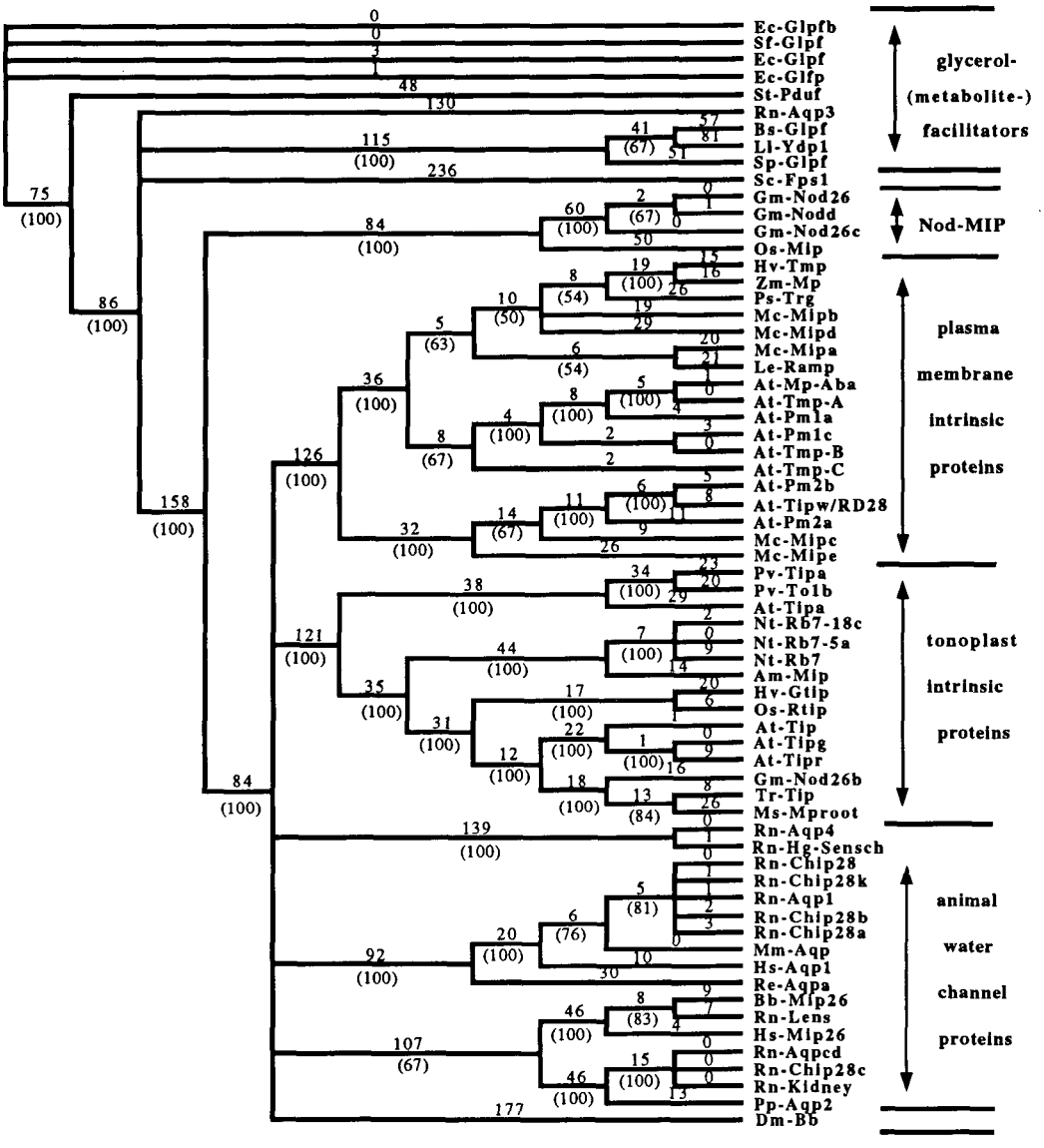

Figure 2. Evolutionary Relationships of the Ice Plant MIP with Channel Proteins and Metabolite Facilitators from a Variety of Organisms.

Protein sequences with EMBL and SwissProt accession numbers are identified by species abbreviation and a mnemonic description followed by the accession number (within parentheses). Parameters employed for parsimony analysis, using PAUP, are described in Methods. The assignment of two subfamilies of plant sequences as tonoplast and plasma membrane channel proteins is based on the functional characterization and localization of some proteins. Ec-Glpfb (P11244), SF-Glpf (P31140), Ec-Glpf (U13915), Ec-Glpf (JU0022), St-Pduf (P37451), Rn-Aqp3 (L35108), Bs-Glpf (P18156), Ll-Ydp1 (P22094), Sp-Glpf (U12567), Sc-Fps1 (P23900), Gm-Nod26 (X04782), Gm-Nodd (JQ2286), Gm-Nod26c (P08995), Os-Mip (D17443), Hv-Tmp (S41194), Zm-Mp (X82633), Ps-Trg (X54357), Mc-Mipb (L36097), Mc-Mipd (U26537), Mc-Mipa (L36095), Le-Ramp (Q08451), At-Mp-Aba (S42556), At-Tmp-A (X68293), At-Pm1a (S44082), At-Pm1c (S44083), At-Tmp-B (X69294), At-Tmp-C (D26609), At-Pm2b (S44085), At-Tipw/RD28 (P30302), At-Pm2a (S44084), Mc-Mipc (L36096), Mc-Mipe (U26538), Pv-Tipa (P23958), Pv-To1b (PQ0185), At-Tipa (P26587), Nt-Rb7-18c (P24422), Nt-Rb7-5a (P21653), Nt-Rb7 (S45406), Am-Mip (P33560), Hv-Gtip (X80266), Os-Rtip (D25534), At-Tip (X72581), At-Tipg (P25818), At-Tipr (P21652), Gm-Nod26b (JQ2287), Tr-Tip (Z29946), Ms-Mproot (L36881), Rn-Aqp4 (U14007), Rn-Hg-Sensch (L27588), Rn-Chip28 (JC1320), Rn-Chip28k (A44395), Rn-Aqp1 (P29975), Rn-Chip28b (S37639), Rn-Chip28a (JT0749), Mm-Aqp (Q02013), Hs-Aqp1 (P29972), Re-Aqpa (L24754), Bb-Mip26 (P06624), Rn-Lens (X53052), Hs-Mip26 (P30301), Rn-Aqpcd (P34080), Rn-Chip28c (JT0750), Rn-Kidney (L28112), Pp-Aqp2 (A53442), and Dm-Bp (P23645). Sequences that share homology are shown, but a functional characterization has not been made in all cases. In addition, it must be remembered that some sequences could be alleles of one gene (for example, three different sequences from *Escherichia coli* are listed, but it is not known whether the *E. coli* genome includes three genes).

amino acids. For another abundant transcript, *MipC*, the C-terminal portion (150 amino acids) of the deduced protein is shown. The third transcript, *MipB*, is at least 10 times less abundant than the two others. *MipB* encodes 285 amino acids.

The evolutionary position of the nucleotide sequences of a number of *Mip*s was analyzed using PAUP (Swofford, 1993). The analysis shown in Figure 2 indicates that the five ice plant sequences belong to a subgroup of *Mip*-related genes whose transcripts are turgor responsive. Related sequences have been detected in Arabidopsis, pea, tomato, and barley. Because several proteins encoded by transcripts in this group have been shown to be plasma membrane located (Daniels et al., 1994; Kammerloher et al., 1994), this group was labeled plasma membrane intrinsic protein (PIP; Figure 2). Within the group, there are uncertainties with respect to alignment, indicated by the low bootstrap values given within parentheses. The group as a whole, however, was separated significantly (100% value) from another subgroup designated TIP because proteins in this group have been shown to be tonoplast located (Johnson et al., 1990; Höfte et al., 1992; Maurel et al., 1993). Distinct from these subgroups are at least three other groups. The first includes functionally characterized animal water channel proteins (Preston and Agre, 1991; Fushimi et al., 1993; Deen et al., 1994). The second group includes sequences that have been found in plant root nodules and in rice roots (Nod-MIP; Figure 2), and the third includes the microbial glycerol facilitator protein, Glpf (Weissenborn et al., 1992). The latter may be better termed metabolite facilitators because this group includes, for example, one rat sequence that by homology had been termed a water channel protein. One Nod-MIP has been shown to be regulated by phosphorylation (Miao et al., 1992). Marginally related are a Drosophila sequence (Dm-Bb; Rao et al., 1990) and a yeast sequence (Sc-FPs1; van Aelst et al., 1991) that cannot be placed according to a function (Figure 2). If we assume that the ice plant sequences encode PIP proteins, there are at least five different PIP-type transcripts, compared to possibly nine PIP-type transcripts in Arabidopsis. In addition, Arabidopsis probably contains four TIP sequences.

Transcript Analysis

RNA gel blot analysis of the ice plant *MipA* and *MipC* indicated that these transcripts are present in roots and leaves, whereas *MipB* could be detected only in roots (Figure 3). When ice plants were stressed, *Mip* transcripts showed different reactions in the presence of NaCl. Transcripts for the relatively low-abundance transcript *MipB* were not noticeably affected by stress, with only a small decline in abundance. Transcript levels for *MipA* and *MipC* declined drastically within < 6 hr after the beginning of stress. Transcript abundance remained low for ~30 hr. After that time period, transcript levels increased again to at least the prestress level. This time course in the decline of expression and recovery was always found. However, the extent of decline and recovery was dependent on plant age (data not shown). *Mip* transcript levels in young plants (< 4 weeks old) were much less susceptible and recovered faster and, occasionally, accumulated to a greater extent after stress, whereas in old plants (> 6 weeks old), transcript levels declined more precipitiously and transcript recovery did not approach prestress levels.

Gene Complexity

Hybridization of *Mip*-related cDNAs to total ice plant DNA under high-stringency conditions (Figure 4) indicated that each transcript is the product of a single gene or of a few similar genes. In total, at least five genes (or small gene families) encoding *Mip* homologs are present in the ice plant genome (~290 megabases; Meyer et al., 1990). Preliminary analysis of genomic clones indicated that some of these genes may be physically linked (C. Michalowski, unpublished data).

In Situ Hybridizations

In situ hybridization was performed with *MipA* and *MipB* to obtain information about cell specificity of expression. Figure 5 provides a histological survey of different sections through roots. Stained sections close to the root tip, < 2 mm from the meristem, indicate the beginning of endodermis formation (Figures 5A and 5B). In Figure 5B, a section after 4′,6-diamidino-2-phenylindole (DAPI) staining and fluorescence photography is shown. It indicates different ploidy levels of the nuclei, with the endodermis nuclei being 2N. Nuclei of senescing root cap

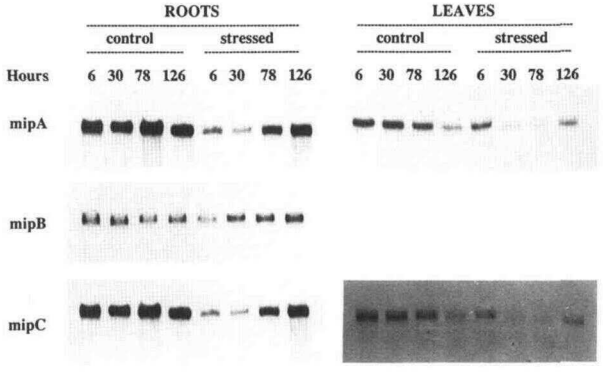

Figure 3. RNA Gel Blot Analysis of Three *Mip*-Related Transcripts Hybridized to Total RNA from Roots and Leaves from Salt-Stressed and Unstressed Ice Plants.

The hybridization signal using ^{32}P-labeled probes for the three transcripts identifies a transcript size of ~1300 nucleotides. Compared are transcript levels from salt-stressed and unstressed plants (hours after stress) in roots and leaves. No signal could be obtained in leaves with the *MipB* probe (20 μg of RNA was loaded in each lane).

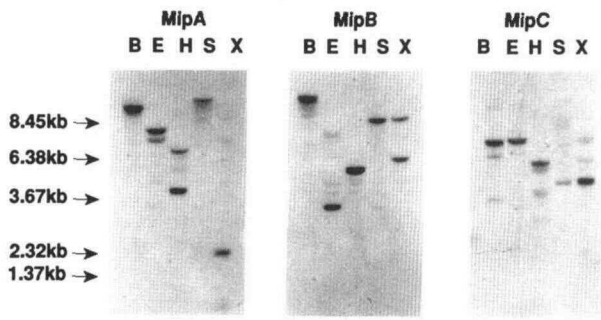

Figure 4. Hybridizations of *MipA*, *MipB*, and *MipC* Probes to Total Ice Plant DNA.

Ten micrograms of total ice plant DNA per lane was restricted with the endonucleases BamHI (B), EcoRI (E), HindIII (H), SalI (S), and XhoI (X). Probes used were from inside the coding regions of the cDNAs. The signals indicate that each cDNA is encoded by a single gene or by a conserved, small gene family. DNA fragment length markers are given at left in kilobases.

cells show condensed chromatin (Figure 5B). The root (not counting root cap cells) at this stage of development consists of an epidermis, four layers of cortex cells, the developing pericycle and endodermis rings of cells, and the developing vascular tissue. Xylem and phloem primordia can be distinguished. Sections through an older root (Figures 5C and 5D) provide an overview of the typical adult root. A central primary xylem (stained dark blue) is surrounded by parenchymatic tissue (stained purple) to which rings of xylem tissue are added successively as secondary growth commences. The xylem and outermost cell layers exhibit high autofluorescence (Figures 5D, 6E, and 6F), which increases when roots are salt stressed (data not shown). Nuclei are typically 4N or 8N in older roots (Figure 5D).

Figure 6 shows the signals after hybridization with either ^{35}S-labeled or digoxigenin-labeled *MipA* transcripts. For each tissue section, hybridization with either the sense (Figures 6A, 6C, and 6E) or antisense (Figures 6B, 6D, and 6F) labeled probes is shown; in most instances, successive sections from one root are compared in these hybridizations. Cells of the epidermis and cells close to the zone of vascular bundle development contain higher signal density than do cortical cells (Figures 6A and 6B). The signal is most concentrated in these cells for the distal ~3 mm of the root tip. This may be due to a density of the cytoplasm in these cells that is higher than that in cortex cells and cells of the root cap, as was seen in a longitudinal section (data not shown). This section indicated above-background hybridization in all cells. Figures 6C and 6D show digoxigenin-labeled signals in cross-sections of a nearly mature root. The signal is most concentrated in cells associated with the outside of the primary xylem. In longitudinal sections of an even older root segment, autofluorescence of the outermost cell layers and xylem is visible (indicated in Figures 6E and 6F), whereas the antisense hybridization also highlights developing xylem tissue (Figure 6F). The root segments shown in Figures 6E and 6F are longitudinal sections at a point of secondary root emergence (upper right corners). At higher magnification, the signal is strongest in developing xylem cells (Figure 7).

Signals obtained with *MipB* were generally fainter than those obtained with *MipA*, which agrees with RNA gel blot hybridizations (Figure 3). A reliable distinction between sense and antisense probes was only possible for the root tip (Figures 8A and 8B). From these hybridizations, it appears that *MipB* is most strongly expressed in the area from the tip of the root to the point at which the vascular bundle is fully differentiated. However, it is impossible to distinguish whether significantly lower expression of this gene is continuing in older parts of the root system.

Some investigations were performed with *MipA* in leaves and stems. Figures 9A and 9B show that hybridization signals appear to be concentrated in vascular tissue. The generally higher contrast in all cells hybridized with the antisense probe (Figure 9B), compared with sense probe hybridizations, seems to indicate that *MipA* is also expressed in mesophyll cells. One notable exception is that we never observed a signal with epidermal cells, particularly not with the large epidermal bladder cells that seem to function as a salt storage organ under salinity stress conditions.

MIP Function

Full-length complementary RNAs of *MipA* and *MipB*, transcribed from cDNAs cloned in vector pXBG-ev1 to assure expression in Xenopus oocytes, were injected into oocytes, and water permeability was measured (Cao et al., 1992; Maurel et al., 1993). Figure 10 shows water uptake 3 days after injection of the oocytes in response to lower osmotic pressure after exchange of the medium. Expression of both MIPA and MIPB indicated that the proteins lead to significant (paired *t* test; 5% level) water uptake over noninjected and mock-injected oocytes, although water permeability is not increased as much as it is after injection of γ-TIP complementary RNA (Maurel et al., 1993; Daniels et al., 1994).

DISCUSSION

Proteins with homology to MIP, a major intrinsic protein originally isolated from mammalian eye lens, are present in plants (Guerrero et al., 1990; Johnson et al., 1990; Höfte et al., 1992; Yamaguchi-Shinozaki et al., 1992). Subfamilies can be distinguished by sequence comparisons that distinguish animal and plant genes and that may distinguish different functions of MIPs (Figure 2). MIPs are biochemically characterized by six membrane-spanning domains forming dimeric or tetrameric complexes (see, for example, Verkman, 1993; Chrispeels and Agre, 1994). For different subgroups, functional information is available. The encoded proteins facilitate transport of water

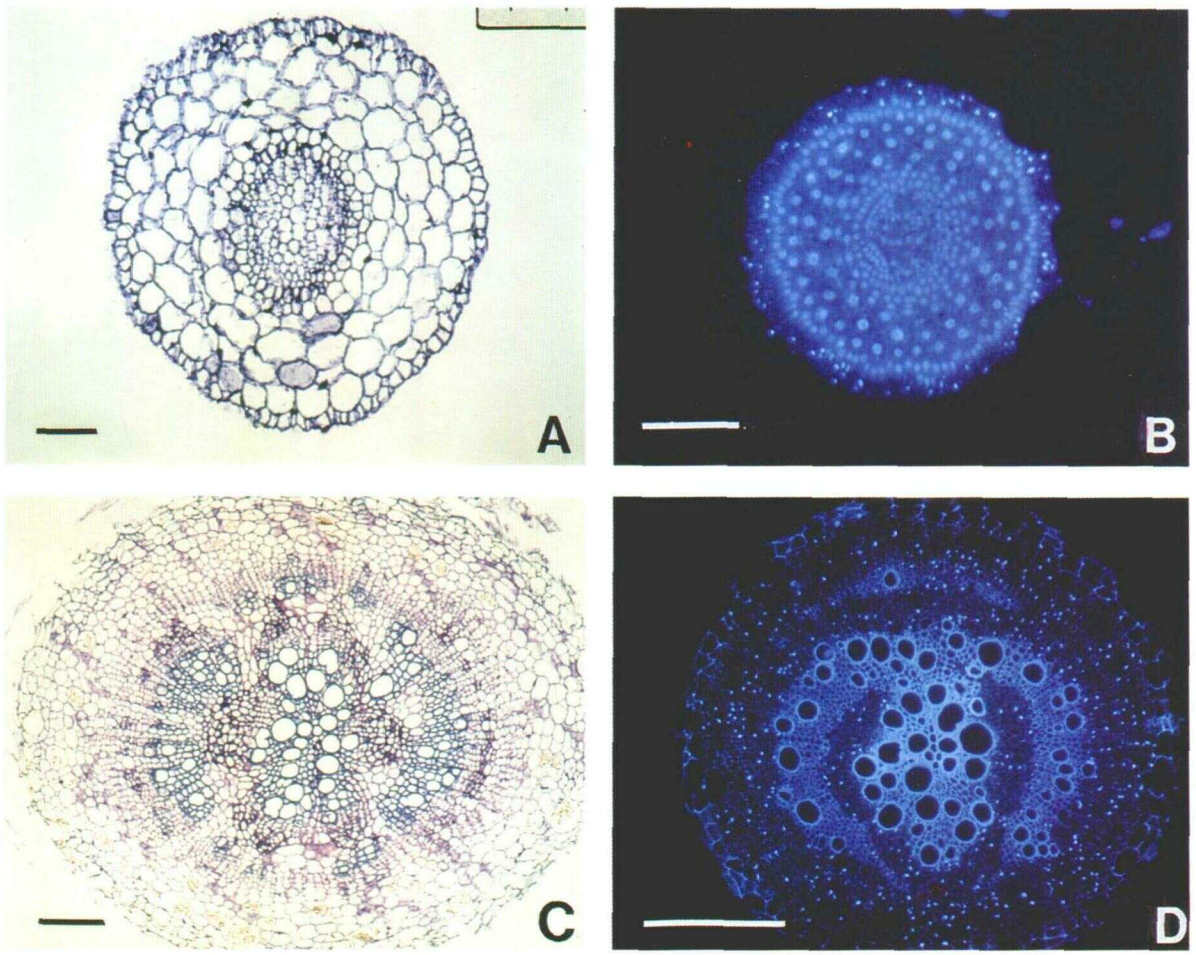

Figure 5. Structure of Ice Plant Roots.

(A) and **(B)** Cross-sections of roots ~2 mm in length.
(C) and **(D)** Cross-sections from root segments >3 cm from the tip.
Sections were stained with toluidine blue in **(A)** and **(C)** or DAPI in **(B)** and **(D)**. In **(A)** and **(B)**, bars = 0.1 mm; in **(C)** and **(D)**, bars = 0.4 mm.

in animals (termed CHIP or WCH-CD) and plants (TIP and PIP), dicarboxylates in nodules (Nod26), water and sodium in animals (MIP), or glycerol (GlpF) or other small straight-chain carbon compounds in bacteria (Reizer et al., 1993; Verkman, 1993; Saier, 1994). Related sequences whose precise functions are not known include a Drosophila sequence (BIB, a neurogenic protein; Rao et al., 1990) and the yeast gene encoding FPS1 (a suppressor of growth deficiency on fermentable sugars; van Aelst et al., 1991).

Several plant MIPs function as aquaporins in the tonoplast (TIP; Maurel et al., 1993) and in the plasma membrane (PIP; Daniels et al., 1994; Kammerloher et al., 1994). As aquaporins, they can be assumed to facilitate osmotic adjustment between the cytoplasm, vacuole, and extracellular space. Use of a unique experimental approach for the isolation of genes encoding plasma membrane proteins resulted in the isolation of several PIPs from Arabidopsis, which may contain 10 *Mip*-related transcripts in total (Kammerloher et al., 1994). According to their sequence characteristics (Figures 1 and 2), the ice plant *Mip* homologs reported here are grouped in the putative PIP subfamily. By using polymerase chain reactions, we have recently isolated additional ice plant transcripts with sequence signatures of TIP subfamily members (M. Ishitani and H.J. Bohnert, unpublished data). The surprising complexity of this gene family may indicate functional complexity in different cells or tissues, developmental specificity of expression, or functional redundancy.

The tissue-specific high expression of the ice plant *Mip* in the epidermis and endodermis of the root tip and their high expression in cells of the differentiating xylem can best be understood by assuming that these proteins are located in the plasma membrane, facilitating symplastic ion or water transport between cells and into the xylem. This location may indicate a function of the encoded MIP in water movement into

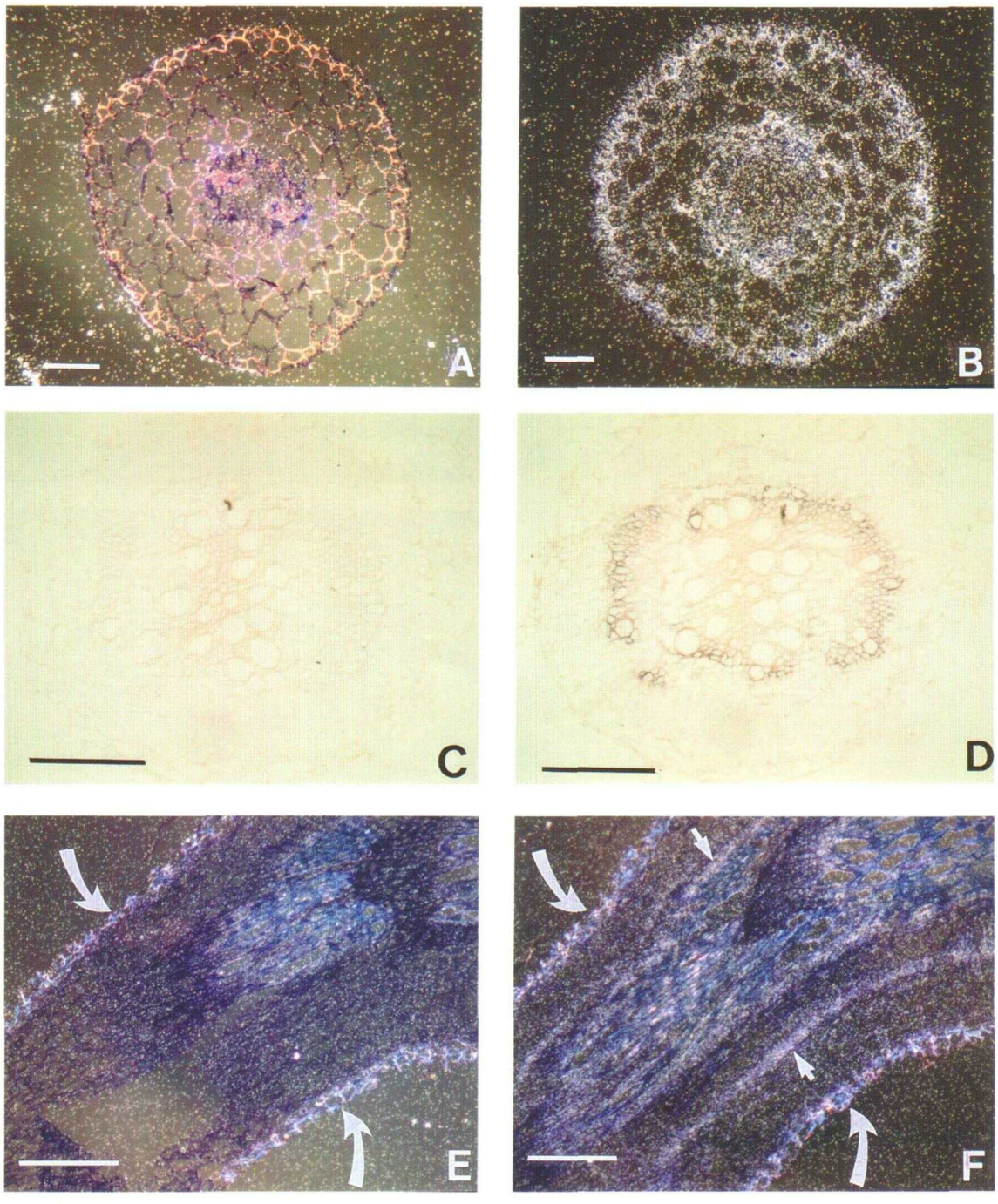

Figure 6. In Situ Hybridization of *MipA* Sense and Antisense Transcripts in Tissue Sections of Roots of Different Developmental Age.

In **(A)**, **(B)**, **(E)**, and **(F)**, the sections were hybridized with sense (**[A]** and **[E]**) or antisense (**[B]** and **[F]**) ^{35}S-labeled probes transcribed with T3 or T7 RNA polymerase from the linearized vector pBluescript KS− containing the *MipA* cDNA. The digoxigenin-labeled *MipA* sense probe was used in **(C)** and the antisense probe was used in **(D)**. When using ^{35}S-labeled probes, the slides were washed after labeling, coated with NTB-2 photographic emulsion (Kodak), and stored at 4°C for 4 weeks before the development of silver grains. The straight arrows in **(F)** point toward the outer layer of the xylem, and the curved arrows in **(E)** and **(F)** indicate tissue autofluorescence. Sections were hybridized with digoxigenin-labeled RNA transcribed by T7 or SP6 RNA polymerase from linearized pSPT18 vectors at a concentration of ~0.7 μg/mL. After hybridization and RNase treatment and washings (see Methods), slides were incubated with 500-fold diluted alkaline phosphatase conjugated to anti-digoxigenin Fab fragments. Color development by alkaline phosphatase was for variable lengths of time, with the maximum being 16 hr.

(A) and **(B)** Sense and antisense strand, respectively; hybridizations with young roots ~2 mm from the tip of the root. Bars = 0.1 mm.

(C) and **(D)** Sense and antisense strand, respectively; hybridizations with root segments ~15 mm from the tip of the root. Bars = 0.5 mm.

(E) and **(F)** Sense and antisense strand, respectively; hybridizations with root segments >20 mm from the tip of the root. Bars = 0.3 mm.

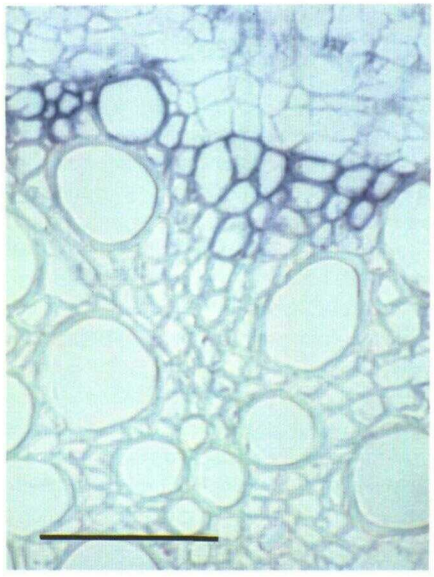

Figure 7. Strongest *MipA* Hybridization Signals in Fully Developed Roots Are Confined to the Youngest Portions of the Xylem.

The primary xylem is located at bottom center. The youngest developing xylem vessels, adjacent to cortical cells (top), show peroxidase staining. Consequently, in old roots that have developed three rings of xylem tissue, there may be hybridization signals in three concentric rings (data not shown). Bar = 0.1 mm.

cells. They may also facilitate entry of water into conducting tissues for long-distance transport (Figure 8). This may be deduced from the expression of *MipA* and *MipB* transcripts in the endodermis of the developing but not totally closed vascular bundle and from the expression of *MipA* in or around xylem strands. Injection of *MipA* and *MipB* cRNA into oocytes resulted in higher water permeability, and some (up to two of four eggs in each experiment) of the injected oocytes actually burst. Water permeability measured 3 days after injection was, however, always more pronounced with γ-TIP (Figure 10).

The ice plant *Mip* transcripts are closely related to Arabidopsis RD28 (Figure 2; Yamaguchi-Shinozaki et al., 1992). In response to drought and salinity stress, however, expression patterns of RD28 transcripts are different from those of the closely related *MipC* and the more distantly related *MipA* and *MipB*. RD28 is barely detectable in unstressed plants (Yamaguchi-Shinozaki et al., 1992). Drought and high salinity lead to an increase in transcript abundance. The ice plant *Mip* homologs, in contrast, are strongly expressed in unstressed plants. As judged by the number of clones from a cDNA library, 35 per 1000 plaques, these transcripts are moderately abundant. Osmotic stress leads to decline and subsequent recovery; this is correlated with the time course of turgor recovery in the whole plant. The kinetics of transcript changes has to be seen in context with other transcripts in the ice plant. Decline of transcript abundance is not simply a consequence of stress, because many transcripts are not affected by 400 mM NaCl (for example, see Cushman et al., 1989; Michalowski et al., 1992; Bohnert et al., 1994).

Apparently, halophytic and glycophytic regulation of MIPs is different. This may have to do with the fact that the ice plant is a sodium includer, able to control influx and deposition of sodium in a tissue-specific and cell-specific manner (Adams et al., 1992). Salinity shock does not produce as severe a water deficit in the ice plant as it does in Arabidopsis, which is largely a sodium excluder. The induction of several plant Mip transcripts by osmotic stress may indicate an adaptive reaction to alleviate water stress, whereas the ice plant must cope primarily with a sudden influx of sodium after salt shock. We think that the different responses to drought and salt shock

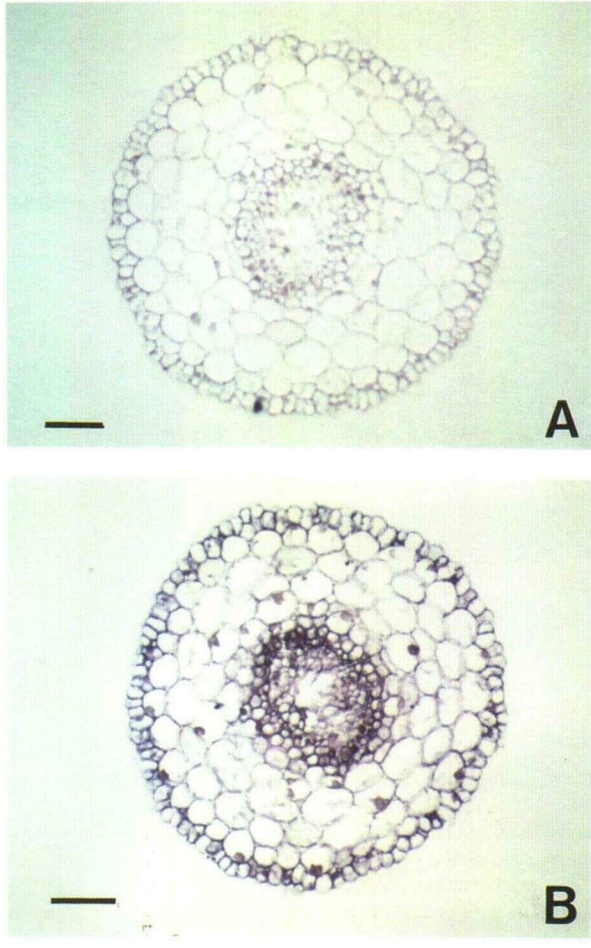

Figure 8. *MipB* Hybridization Signals Are Confined to Root Tips.

(A) Sense hybridization.
(B) Antisense hybridization.
Shown are cross-sections through young roots < 2 mm from the tip. Young root tissue was the only tissue in which a hybridization signal could be demonstrated reliably. Bars = 0.15 mm.

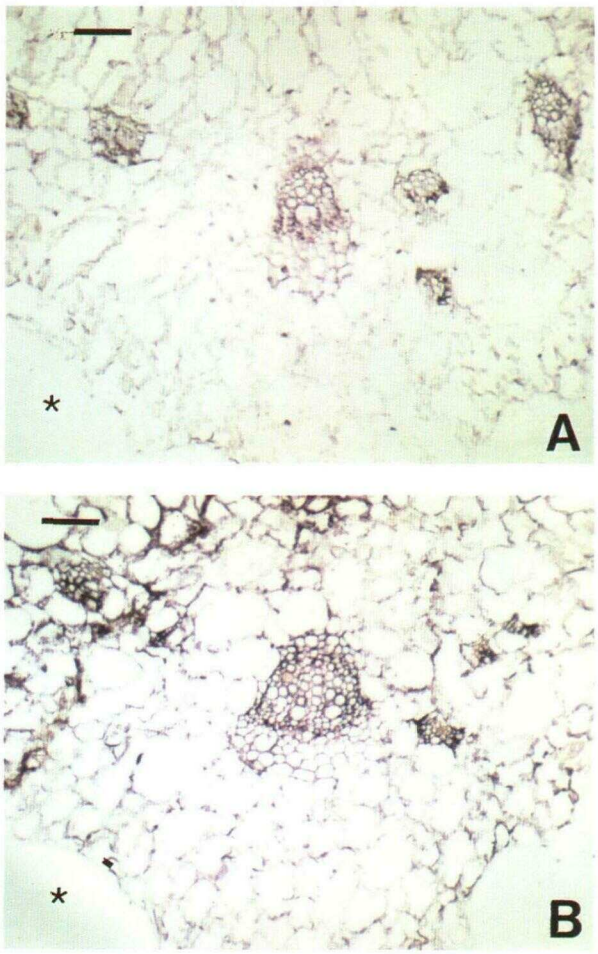

Figure 9. *MipA* Hybridization Signals in Leaves.

Cross-sections through the base of a leaf, close to the petiole, are shown.

(A) Hybridization analysis with a sense probe.

(B) Hybridization analysis with an antisense probe.

It appears that all cells carry a signal (as shown in **[B]**), although there are differences in different parts of the leaf. Not highlighted are the epidermal bladder cells that line the rim of the leaf (indicated by asterisks). Bars = 0.1 mm.

reveal a significant difference between glycophytic and halophytic plants. However, in both plants it must still be shown that the changes in transcript levels under stress lead to changes in protein amount. For the ice plant, MIPA and MIPB functions have been established, but tissue-specific expression of the remaining presumptive PIP must be investigated.

The results add tissue- and cell-specific expression to our knowledge of plant *Mip* homologs. A similar analysis has been provided for a tobacco transcript, the *Mip*-related TobRB7. This analysis focused on *cis*-acting elements important in root-specific gene expression (Yamamoto et al., 1991). Examination of the in situ hybridization data with *MipA* and *MipB* clearly establishes specific tissues and cells within these tissues as strongly expressing *Mip*-related genes. In addition to those cells, we believe there is much weaker expression of the genes in other tissues and cells. This we deduced from the antisense hybridization signals, which always highlight all cells in a more pronounced fashion than do the sense strand hybridizations. In addition to the strong signal in cells surrounding the vascular bundles, the antisense contrast is enhanced in mesophyll cells (see, for example, Figure 9). The epidermis and epidermal bladder cells, however, are not highlighted, which may indicate at least one tissue in which *MipA* is not found.

The importance of cell-specific PIP expression in general (and for salinity tolerance of the ice plant in particular) is not immediately clear. Both Arabidopsis and the ice plant express several transcripts that are members of an ancient gene family. Obviously, functional diversification has produced the extant complexity. We expect that gene complexity reflects different metabolite transport activities or different adaptation to osmotic challenges. The genes may also have been duplicated in response to the different requirements of specialized tissues, for example, to accommodate seed germination, symplastic metabolite and water entry in the root, long-distance transport, guard cell volume regulation, rapid cell expansion during flower emergence, guttation, and nectar secretion. The involvement of MIP homologs in such diverse functions suggests they play a fundamental role in establishing plant form and function. Their cell-specific expression, regulation of activity, and consequences of gene inactivations are important to study.

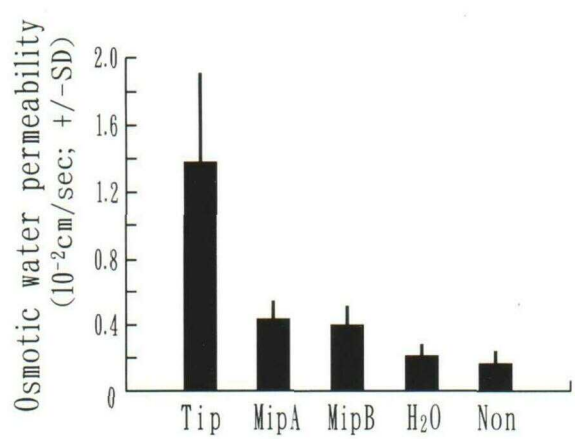

Figure 10. Osmotic Water Permeability in Injected Oocytes Expressing *MipA* and *MipB*.

Oocytes were injected with complementary RNA of γ-*Tip* (Tip; Maurel et al., 1993) (n = 4), *MipA* (n = 4), *MipB* (n = 4), or distilled water (n = 5). Non indicates oocytes that were not injected (n = 5). Three days after injection, the oocytes were subjected to a hypotonic treatment. Oocytes that did not show any reaction were not included in the data. Reactions varied between the two batches of oocytes used. Statistical analysis by paired t tests indicated that the injected *MipA* and *MipB* transcripts led to significantly increased water permeability (5% level).

We have focused on root-specific gene expression in the ice plant under water and sodium stress. We expected that roots under osmotic stress would reveal mechanisms through which the halophytic ice plant is able to tolerate salinity stress severe enough to eliminate most other plants. At 400 mM NaCl in the medium surrounding roots, the osmotic pressure is high enough to desiccate the tissue, necessitating the presence or buildup of defense mechanisms. One mechanism may be salt exclusion or controlled uptake of Na^+, accompanied by internal osmolyte accumulation (Vernon and Bohnert, 1992) that could lead to increased uptake of water. Should aquaporins be a main route for water uptake in plants, control of *Mip* expression, the amount of aquaporins in membranes, and regulation of their activity, for example, by phosphorylation (Miao et al., 1992; Daniels et al., 1994), might be crucial not only under normal growth but equally under osmotic stress conditions. To make sodium exclusion a viable strategy, reducing aquaporin amount or activity following stress would buy time and allow for internal osmotic adjustment. That aquaporins contribute significantly to water movement has recently been shown (Kaldenhoff et al., 1995). Isolated protoplasts expressing antisense PIP transcripts contained reduced amounts of PIP protein. After transfer into water, bursting of cells was significantly retarded compared with results involving control protoplasts.

Until recently, facilitated movement of water has been documented for specialized animal cells, for example, in mammalian kidneys (Fushimi et al., 1993; Zhang et al., 1993; Deen et al., 1994). The animal aquaporins constitute pores, which may be regulated, through which water is channeled without being connected to net ion flow (Verkman, 1993; Zeuthen and Stein, 1994). The characterization of plant aquaporins (Maurel et al., 1993; Daniels et al., 1994; Kammerloher et al., 1994) has provided an understanding of their functioning in general. Aquaporins may also highlight a strategy plants use to continue to take up water under stress conditions. As observed in the ice plant, several of the transcripts have been shown to be regulated by turgor pressure and osmotic stresses (for example, see Guerrero et al., 1990; Yamaguchi-Shinozaki et al., 1992; Fray et al., 1994). Although regulated, facilitated water movement may be a strategy to cope with osmotic shock.

METHODS

Plant Material

Plants (*Mesembryanthemum crystallinum*) were grown from seed as described by Ostrem et al. (1987). Plants used for cDNA library construction, RNA analysis, and in situ hybridization were transferred to hydroponic tanks (Vernon and Bohnert, 1992) ~10 days after seedling germination in vermiculite. Plants used for cDNA library construction and RNA analysis were subjected to 400 mM NaCl stress when the plants were 6 weeks old. Unstressed controls for each experiment were grown alongside stressed plants and were harvested at the same time.

cDNA Library Construction and Differential Screening

Total mRNA was extracted from salt-stressed or unstressed roots of common ice plants. Poly(A)$^+$ mRNA was prepared as described previously (Ostrem et al., 1987). The cDNA library from RNA of stressed roots was constructed in λZAPII (Stratagene) and screened by differential hybridization, with first-strand cDNA synthesized from poly(A)$^+$ mRNA isolated from stressed and unstressed plants.

DNA Sequence Analysis

Nucleotide sequences of *Mip* (for major intrinsic protein)–related transcripts were obtained by dideoxy sequencing of overlapping deletion clones, subclones using existing restriction sites, or selected full-length cDNAs cloned into pBluescript II KS+ and KS– plasmids (Stratagene). Sequence comparisons with sequences in the EMBL and SwissProt data bases (see legend of Figure 2 for accession numbers) were performed using Genetics Computer Group (Madison, WI) programs (Devereux et al., 1985; Higgins and Sharp, 1989). Parsimony analysis was done using PAUP, version 3.1 (Swofford, 1993). The heuristic option of PAUP was used with simple addition of sequences and TBR branch swapping. Analyses were performed repeatedly, with the order of sequence additions varied. Sequences were trimmed so that 5′ or 3′ extensions of individual sequences were removed. Internal extensions in some sequences, which were identified by multiple alignment programs, were treated as missing characters in the other sequences. The number of bootstrap replicates was set to 100. The resulting tree is unrooted. The final alignment is available upon request.

RNA Gel Blot Analysis

Total RNA was isolated from leaves and roots as described previously (Vernon and Bohnert, 1992). Ten micrograms of LiCl-purified total RNA was resolved on formaldehyde–agarose gels and transferred to Zetaprobe membranes (Bio-Rad). Blots were probed with ^{32}P-labeled probes derived from various *Mip*-related clones. After hybridization, blots were washed under high-stringency conditions (40 mM Na_2HPO_4, pH 7.2, 1 mM EDTA, 1% SDS at 65°C) and subjected to autoradiography.

Tissue Preparation and in Situ Hybridizations

Fresh root and leaf tissues of the ice plant were fixed with 2% glutaraldehyde in 0.05 M sodium cacodylate buffer at 4°C for 1 to 2 hr, dehydrated in an ethanol series, and infiltrated with paraffin at room temperature. The embedded tissue was sectioned into 6- to 10-μm-thick slices and fixed on poly-L-lysine–coated glass slides. These slides were used for histological observation, 4′,6-diamidino-2-phenylindole (DAPI) staining, and in situ hybridization. For histological observation, sections were stained with toluidine blue (Clark et al., 1992). DAPI staining was performed according to DeRocher et al. (1990). In situ hybridization with ^{35}S-labeled probes was performed as described previously (Clark et al., 1992). The slides were hybridized with either antisense or sense strands of *MipA* RNA probes transcribed by T3 or T7 RNA polymerase from linearized pBluescript KS– harboring the cDNA. The slides were then washed and coated with NTB-2 photographic emulsion (Kodak, Rochester, NY) and exposed at 4°C for 4 weeks. After the development of silver grains, the slides were stained with toluidine blue for histological observations.

In situ hybridizations with digoxigenin-labeled probes were performed as described by McKhann and Hirsch (1993) with slight modifications. The digoxigenin-labeled probes were transcribed by T7 or SP6 RNA polymerase from linearized pSPT18 harboring the cDNAs. After hybridization, the slides were treated with RNase A (200 μg/ mL) at 37°C, then washed twice with RNase buffer (100 mM Tris-HCl, pH 7.5, 0.5 M NaCl) at 37°C. Following a series of washes in 1 × SSC (1 × SSC is 0.15 M NaCl, 0.015 M sodium citrate; McKhann and Hirsch, 1993), the sections were incubated with a 500-fold diluted alkaline phosphatase–conjugated anti-digoxigenin Fab fragment. After color development for up to 16 hr, sections were photographed. All observations were made using an Axiophot fluorescence microscope (Zeiss, Jena, Germany).

DNA Gel Blot Hybridization

Total DNA was isolated from leaves as described previously (Vernon and Bohnert, 1992). Ten micrograms of DNA per lane was digested with the restriction endonuclease indicated (Figure 4) and separated on 0.7% agarose gels; the DNA fragments were then transferred to Zetaprobe (Bio-Rad) membranes. Filters were prehybridized and hybridized with ^{32}P-labeled inserts of the cDNA clones as described previously (Vernon and Bohnert, 1992). After hybridization, blots were washed under high-stringency conditions as described for RNA gel blot hybridization analysis.

Construction of Oocyte Expression Vectors and Complementary RNA Synthesis

MipA was removed from its vector by XbaI digestion and *MipB* by digestion with EcoRI and EcoRV. After fill-in with the Klenow fragment of DNA polymerase I, each fragment was inserted into the blunt-ended BglII site of vector pXBG-ev1 (a pSP64T-derived pBluescript-type vector into which Xenopus β-globin 5′ and 3′ untranslated sequences have been inserted; Preston et al., 1992). Constructs were linearized with PstI, and complementary RNA was synthesized (Cao et al., 1992) in vitro using T3 RNA polymerase, 0.4 mM each ribonucleotide-5′-triphosphates, and 0.4 mM m^7GpppG for mRNA capping (Pharmacia, Uppsala, Sweden). After ethanol precipitation, synthesis products were suspended in diethylpyrocarbonate-treated H_2O at a final concentration of 1 mg/mL. Complementary RNA of the tonoplast intrinsic protein γ-TIP (1 mg/mL) was kindly provided by M.J. Daniels (University of California at San Diego, La Jolla).

Oocyte Preparations and Injections

Oocytes were prepared as described previously (Cao et al., 1992) and incubated in Barth's solution (88 mM NaCl, 1 mM KCl, 2.4 mM $NaHCO_3$, 10 mM Hepes-NaOH, 0.33 mM $Ca[NO_3]_2$, 0.41 mM $CaCl_2$, 0.82 mM $MgSO_4$, pH 7.4) supplemented with gentamycin (1 mL stock solution per liter; Sigma) 1 day before microinjection. Two different batches of oocytes were injected with 50 nL of complementary RNA (20 to 50 ng) or with distilled H_2O. Three days after injection they were transferred from Bath's solution (200 mosmol/kg) to diluted Barth's solution (40 mosmol/kg). Changes in cell volume were calculated from changes in cell diameter documented by photographs at 5- to 20-sec intervals. Water permeability coefficients were calculated according to Maurel et al. (1993).

ACKNOWLEDGMENTS

We are grateful to Anna Clark for help with in situ hybridizations, and we thank Richard G. Jensen and Pat Adams for discussions and data on polyol production and ion measurements. We thank Don Nelson for suggestions on the manuscript and Maarten Chrispeels for making results available prior to publication. We thank Julian I. Schroeder and acknowledge his support by the U.S. Department of Energy (Grant No. De-FG03-94-ER20148). W.B.K. is a graduate student in the laboratory of Julian Schroeder. This work was supported by the U.S. Department of Agriculture (Plant Responses to the Environment) and by the Arizona Agricultural Experiment Station. S.Y. has been supported by Japan Tobacco Inc. through a graduate fellowship. M.K. acknowledges support by the Ministry of Education, Science, and Culture, Japan.

Received February 22, 1995; accepted May 16, 1995.

REFERENCES

Adams, P., Thomas, J.C., Vernon, D.M., Bohnert, H.J., and Jensen, R.G. (1992). Distinct cellular and organismic responses to salt stress. Plant Cell Physiol. **33,** 1215–1223.

Bohnert, H.J., Thomas, J.C., DeRocher, E.J., Michalowski, C.B., Breiteneder, H., Vernon, D.M., Deng, W., Yamada, S., and Jensen, R.G. (1994). Responses to salt stress in the halophyte *Mesembryanthemum crystallinum*. In Biochemical and Cellular Mechanisms of Stress Tolerance in Plants, J.H. Cherry, ed (Berlin: Springer-Verlag), pp. 415–428.

Cao, Y., Anderova, M., Crawford, N.M., and Schroeder, J.I. (1992). Expression of an outward-rectifying potassium channel from maize mRNA and complementary RNA in Xenopus oocytes. Plant Cell **4,** 961–969.

Chrispeels, M.J., and Agre, P. (1994). Aquaporins: Water channel proteins of plant and animal cells. Trends Biol. Sci. **19,** 421–425.

Clark, A.M., Verbeke, J.A., and Bohnert, H.J. (1992). Epidermis-specific gene expression in Pachyphytum. Plant Cell **4,** 1189–1198.

Cushman, J.C., and Bohnert, H.J. (1995). Transcriptional activation of CAM-genes during development and environmental stress. In Crassulacean Acid Metabolism: Biochemistry, Ecophysiology and Evolution, K. Winter, A.P. Smith, and J.A.C. Smith, eds (Heidelberg: Springer-Verlag), in press.

Cushman, J.C., Meyer, G., Michalowski, C.B., Schmitt, J.M., and Bohnert, H.J. (1989). Salt stress leads to differential expression of two isogenes of phosphoenolpyruvate carboxylase during Crassulacean acid metabolism induction in the common ice plant. Plant Cell **1,** 715–725.

Daniels, M.J., Mirkov, T.E., and Chrispeels, M.J. (1994). The plasma membrane of *Arabidopsis thaliana* contains a mercury-insensitive aquaporin that is a homolog of the tonoplast water channel protein TIP. Plant Physiol. **106,** 1325–1333.

Deen, P.M.T., Verdijk, M.A.J., Knoers, N.V.A.M., Wierenga, B., Monnens, L.A.H., van Os, C.H., and van Oost, B.A. (1994). Requirement of human renal water channel aquaporin-2 for vasopressin-dependent concentration of urine. Science **264,** 92–95.

Delauney, A.J., and Verma, D.P.S. (1993). Proline biosynthesis and osmoregulation in plants. Plant J. **4,** 215–223.

DeRocher, E.J., Harkins, K.R., Galbraith, D.W., and Bohnert, H.J. (1990). Developmentally regulated systemic endopolyploidy in succulents with small genomes. Science **250,** 99–101.

Devereux, J., Haeberli, P., and Smithies, O. (1985). A comprehensive set of sequence analysis programs for the VAX. Nucleic Acids Res. **12,** 387–393.

Fray, R.G., Wallace, A., Grierson, D., and Lycett, G.W. (1994). Nucleotide sequence and expression of a ripening and water stress–related cDNA from tomato with homology to the MIP class of membrane channel proteins. Plant Mol. Biol. **24,** 539–543.

Fushimi, K., Uchida, S., Hara, Y., Hirata, Y., Marumo, F., and Sasaki, S. (1993). Cloning and expression of apical membrane water channel of rat kidney collecting tubule. Nature **361,** 549–552.

Gorin, M.B., Yancey, S.B., Cline, J., Revel, J.P., and Horwitz, J. (1984). The major intrinsic protein (MIP) of the bovine lens fiber membrane: Characterization and structure based on cDNA cloning. Cell **39,** 49–59.

Guerrero, F.D., Jones, J.T., and Mullet, J.E. (1990). Turgor-responsive gene transcription and RNA levels increase rapidly when pea shoots are wilted: Sequence and expression of three inducible genes. Plant Mol. Biol. **15,** 11–26.

Higgins, D.G., and Sharp, P.M. (1989). Fast and sensitive multiple sequence alignments on a microcomputer. CABIOS Commun. **5,** 151–153.

Höfte, H., Hubbard, L., Reizer, J., Ludevid, D., Herman, E.M., and Chrispeels, M.J. (1992). Vegetative and seed-specific forms of tonoplast intrinsic protein in the vacuolar membrane of *Arabidopsis thaliana.* Plant Physiol. **99,** 561–570.

Johnson, K.D., Höfte, H., and Chrispeels, M.J. (1990). An intrinsic tonoplast protein of protein storage vacuoles in seeds is structurally related to a bacterial solute transporter (GlpF). Plant Cell **2,** 525–532.

Kaldenhoff, R., Kölling, A., Meyers, J., Karmann, U., Ruppel, G., and Richter, G. (1995). The blue light–responsive *AthH2* gene of *Arabidopsis thaliana* is primarily expressed in expanding as well as differentiating cells and encodes a putative channel protein of the plasmalemma. Plant J. **7,** 87–95.

Kammerloher, W., Fischer, U., Piechottka, G.P., and Schäffner, A.R. (1994). Water channels in the plasma membrane cloned by immunoselection from a mammalian expression system. Plant J. **6,** 187–199.

Maurel, C., Reizer, J., Schroeder, J.I., and Chrispeels, M.J. (1993). The vacuolar membrane protein γ-TIP creates water specific channels in Xenopus oocytes. EMBO J. **12,** 2241–2247.

McCue, K.F., and Hanson, A.D. (1990). Drought and salt tolerance: Toward understanding and application. Trends Biotechnol. **8,** 358–362.

McKhann, H.I., and Hirsch, A.M. (1993). In situ localization of specific mRNAs in plant tissues. In Methods in Plant Molecular Biology and Biotechnology, B.R. Glick and J.E. Thompson, eds (Boca Raton, FL: CRC Press), pp. 179–205.

Meyer, G., Schmitt, J.M., and Bohnert, H.J. (1990). Direct screening of a small plant genome: Estimation of the magnitude of plant gene expression changes during adaptation to high salt. Mol. Gen. Genet. **224,** 347–356.

Miao, G.H., Hong, Z., and Verma, D.P.S. (1992). Topology and phosphorylation of soybean Nodulin-26, an intrinsic protein of the peribacteroid membrane. J. Cell Biol. **118,** 481–490.

Michalowski, C.B., DeRocher, E.J., Bohnert, H.J., and Salvucci, M.E. (1992). Phosphoribulokinase from ice plant: Transcription, transcripts and protein expression during environmental stress. Photosyn. Res. **31,** 127–138.

Ostrem, J.A., Olsen, S.W., Schmitt, J.M., and Bohnert, H.J. (1987). Salt stress increases the level of translatable mRNA for phosphoenolpyruvate carboxylase in *Mesembryanthemum crystallinum.* Plant Physiol. **84,** 1270–1275.

Pao, J.M., Wu, L.F., Höfte, H., Chrispeels, M.J., Sweet, G., Sandal, N.N., and Saier, M.H., Jr. (1991). Evolution of the MIP family of integral membrane transport proteins. Mol. Microbiol. **5,** 33–37.

Preston, G.M., and Agre, P. (1991). Isolation of the cDNA for erythrocyte integral membrane protein of 28 kilodaltons: Members of an ancient channel family. Proc. Natl. Acad. Sci. USA **88,** 11110–11114.

Preston, G.M., Carroll, T.P., Guggino, W.B., and Agre, P. (1992). Appearance of water channels in Xenopus oocytes expressing red cell CHIP28 protein. Science **256,** 385–387.

Rao, Y., Jan, L.Y., and Jan, N. (1990). Similarity of the product of the *Drosophila* neurogenic gene big brain to transmembrane channel proteins. Nature **345,** 163–167.

Reizer, J., Reizer, A., and Saier, M.H., Jr. (1993). The MIP family of integral membrane channel proteins: Sequence comparisons, evolutionary relationships, reconstructed pathway of evolution and proposed functional differentiation of the two repeated halves of the proteins. Crit. Rev. Biochem. Mol. Biol. **28,** 235–257.

Saier, M.H., Jr. (1994). Computer-aided analyses of transport protein sequences: Gleaning evidence concerning function, structure, biogenesis, and evolution. Microbiol. Rev. **58,** 71–93.

Swofford, D.L. (1993). PAUP: Phylogenetic Analysis Using Parsimony, version 3.1. (Champaign, IL: Illinois Natural History Survey).

Tarczynski, M.C., Jensen, R.G., and Bohnert, H.J. (1993). Stress protection of transgenic tobacco by production of the osmolyte mannitol. Science **259,** 508–509.

Thomas, J.C., McElwain, E.F., and Bohnert, H.J. (1992). Convergent induction of osmotic stress responses. Plant Physiol. **100,** 416–423.

van Aelst, L., Hohmann, S., Zimmermann, F.K., Jans, A.W., and Thevelein, J.M. (1991). A yeast homologue of the bovine lens fiber *Mip* gene family complements the growth defect of a *Saccharomyces cerevisiae* mutant on fermentable sugars but not its defect in glucose-induced RAS-mediated cAMP signaling. EMBO J. **10,** 2095–2104.

Verkman, A.S., ed (1993). Water Channels. (Austin, TX: R.G. Landes Co.).

Vernon, D.M., and Bohnert, H.J. (1992). A novel methyl transferase induced by osmotic stress in the facultative halophyte *Mesembryanthemum crystallinum.* EMBO J. **11,** 2077–2085.

Vernon, D.M., Ostrem, J.A., and Bohnert, H.J. (1993). Stress perception and response in a facultative halophyte: The regulation of salinity-induced genes in *Mesembryanthemum crystallinum.* Plant Cell Environ. **16,** 437–444.

Weissenborn, D.L., Wittekind, N., and Larson, T.J. (1992). Structure and regulation of the *glpFK* operon encoding glycerol diffusion facilitator and glycerol kinase of *Escherichia coli* K-12. J. Biol. Chem. **267,** 6122–6131.

Yamaguchi-Shinozaki, K., Koizumi, M., Urao, S., and Shinozaki, K. (1992). Molecular cloning and characterization of 9 cDNAs for genes that are responsive to desiccation in *Arabidopsis thaliana*: Sequence analysis of one cDNA that encodes a putative transmembrane channel protein. Plant Cell Physiol. **33,** 217–224.

Yamamoto, Y.T., Taylor, C.G., Acedo, G.N., Cheng, C.-L., and Conkling, M.A. (1991). Characterization of *cis*-acting sequences regulating root-specific gene expression in tobacco. Plant Cell **3,** 371–382.

Yancey, P.H., Clark, M.E., Hand, S.C., Bowlus, R.D., and Somero, G.N. (1982). Living with water stress: Evolution of osmolyte systems. Science **217,** 1214–1217.

Zeuthen, T., and Stein, W.D. (1994). Co-transport of salt and water in membrane proteins: Membrane proteins as osmotic engines. J. Membr. Biol. **137,** 179–195.

Zhang, R., Skach, W., Hasegawa, H., van Hoek, A.N., and Verkman, A.S. (1993). Cloning, functional analysis and cell localization of a kidney proximal tubule water transporter homologous to CHIP28. J. Cell Biol. **120,** 359–369.